



Streptococcus sanguinis Noncoding *cia*-Dependent Small RNAs Negatively Regulate Expression of Type IV Pilus Retraction ATPase PilT and Biofilm Formation

Chiaki Ota,^a Hirobumi Morisaki,^b Masanobu Nakata,^c Takafumi Arimoto,^b Haruka Fukamachi,^b Hideo Kataoka,^b Yoshiko Masuda,^d Noriyuki Suzuki,^a Takashi Miyazaki,^a Nobuo Okahashi,^e Hirotaka Kuwata^b

^aDivision of Endodontology, Department of Conservative Dentistry, Showa University School of Dentistry, Tokyo, Japan

^bDepartment of Oral Microbiology and Immunology, Showa University School of Dentistry, Tokyo, Japan

^cDepartment of Oral and Molecular Microbiology, Graduate School of Dentistry, Osaka University, Osaka, Japan

^dDivision of Endodontics and Operative Dentistry, Department of Restorative and Biomaterials Sciences, Meikai University School of Dentistry, Saitama, Japan

^eCenter for Frontier Oral Science, Osaka University Graduate School of Dentistry, Osaka, Japan

ABSTRACT Small noncoding RNAs (sRNAs) have been identified as important regulators of gene expression in various cellular processes. *cia*-dependent small RNAs (csRNAs), a group of sRNAs that are controlled by the two-component regulatory system CiaRH, are widely conserved in streptococci, but their targets have been identified only in *Streptococcus pneumoniae*. *Streptococcus sanguinis*, a pioneer colonizer of teeth and one of the most predominant bacteria in the early oral biofilm, has been shown to have six csRNAs. Using computational target prediction and the luciferase reporter assay, we identified *pilT*, a constituent of the type IV pilus operon, as a negative regulatory target for one of the csRNAs, namely, csRNA1-1, in *S. sanguinis*. RNA-RNA electrophoretic mobility shift assay using a nucleotide exchange mutant of csRNA1-1 revealed that csRNA1-1 binds directly to *pilT* mRNA. In addition, csRNA1-1 and csRNA1-2, a putative gene duplication product of csRNA1-1 that is tandemly located in the *S. sanguinis* genome, negatively regulated *S. sanguinis* biofilm formation. These results suggest the involvement of csRNAs in the colonization step of *S. sanguinis*.

KEYWORDS CiaRH, PilT, *Streptococcus sanguinis*, csRNA, type IV pili

Streptococcus sanguinis, a Gram-positive facultative anaerobe, is a commensal pioneer colonizer in oral biofilm formation and is also implicated in infective endocarditis. *S. sanguinis* adheres directly to saliva-coated teeth by a variety of mechanisms, including interaction with salivary components, e.g., α -amylase and secretory immunoglobulin A complex (1). After adherence, *S. sanguinis* provides a new scaffold for attachment and induces environmental changes, which include extracellular polysaccharide synthesis, H₂O₂ production, and DNA release (2, 3, 4). These changes affect the colonization of other oral microorganisms that constitute the oral biofilm. While various factors associated with the biofilm-forming ability of *S. sanguinis* have been identified, regulatory mechanisms of colonization and biofilm formation are extremely complex and still unclear.

In recent years, bacterial noncoding small RNAs (sRNAs) have received great attention because of their important roles in cellular processes, including adaptive responses and colonization (5). Bacterial sRNAs can control gene function using multiple molecular mechanisms to regulate the expression of target genes, including direct binding to complementary nucleotide sequences within target mRNA (6, 7). The best-characterized streptococcal sRNA is FasX of *Streptococcus pyogenes*.

Received 5 December 2017 Accepted 6 December 2017

Accepted manuscript posted online 20 December 2017

Citation Ota C, Morisaki H, Nakata M, Arimoto T, Fukamachi H, Kataoka H, Masuda Y, Suzuki N, Miyazaki T, Okahashi N, Kuwata H. 2018. *Streptococcus sanguinis* noncoding *cia*-dependent small RNAs negatively regulate expression of type IV pilus retraction ATPase PilT and biofilm formation. Infect Immun 86:e00894-17. <https://doi.org/10.1128/IAI.00894-17>.

Editor Andreas J. Bäuml, University of California, Davis

Copyright © 2018 American Society for Microbiology. All Rights Reserved.

Address correspondence to Hirobumi Morisaki, morisaki@dent.showa-u.ac.jp.

TABLE 1 Transcriptional regulation of csRNAs by the CiaRH system

Target	Fold change in expression ^a		
	WT mock	Δ <i>ciaRH</i> mock	Δ <i>ciaRH</i> +pVACiaRH
csRNA1-1	1 \pm 0.060	0.001 \pm 0.0003 ^b	0.64 \pm 0.154
csRNA1-2	1 \pm 0.165	0.015 \pm 0.017 ^b	1.67 \pm 0.639
csRNA1-3	1 \pm 0.102	0.108 \pm 0.060 ^b	1.47 \pm 0.097
csRNA2	1 \pm 0.343	0.008 \pm 0.027 ^b	1.90 \pm 0.716
csRNA7	1 \pm 0.181	0.015 \pm 0.027 ^b	1.47 \pm 0.561
csRNA8	1 \pm 0.138	0.997 \pm 0.342	1.34 \pm 0.253

^aMean values and standard deviations from three independent cultures are presented.

^b $P < 0.01$.

FasX positively or negatively regulates the expression of *S. pyogenes* virulence factors, including streptokinase, collagen-binding pili, and fibronectin-binding proteins (PrtF1 and PrtF2), through interaction with the 5' untranslated region (UTR) of target mRNAs (8, 9, 10, 11). Since these posttranscriptional levels of regulation result in a quicker effect than transcriptional regulation, sRNAs are mainly associated with the fine-tuning of metabolic processes or stress adaptation.

Two-component systems (TCSs) are bacterial transcriptional regulatory systems that play important roles in the bacterial response to environmental changes (12, 13). A conventional TCS is composed of a transmembrane sensor histidine kinase and a cytoplasmic response regulator. When sensing an extracellular signal, the sensor kinase autophosphorylates on a histidine residue and then transfers the phosphate group to the response regulator, which in turn acts as a transcription factor of target genes. The first characterized TCS in streptococci, namely, the CiaRH system, which is composed of CiaH histidine kinase and a CiaR response regulator, was identified in a search for spontaneous cefotaxime-resistant mutants of *Streptococcus pneumoniae* (14). In addition to β -lactam antibiotic resistance, CiaRH has been implicated in genetic competence, host colonization, bacteriocin production, and virulence (15, 16, 17, 18). A search for CiaR target genes in *S. pneumoniae* identified 15 promoters, which control the expression of 24 genes. Five of these promoters control sRNA transcription and are designated *cia*-dependent small RNAs (csRNAs) (19). BLAST searches using the five csRNAs from *S. pneumoniae* as a query revealed that all streptococcal genomes sequenced thus far contain *csRNA* genes (20). Among the streptococcal genomes searched in the study, *S. sanguinis* has been shown to express six csRNAs, namely, csRNA1-1, csRNA1-2, csRNA1-3, csRNA2, csRNA7, and csRNA8. To date, the functions of these csRNAs have not been elucidated.

In the present study, we performed a computational target search for csRNAs in *S. sanguinis*. We identified *pilT*, a constituent of the type IV pilus gene cluster, as a target gene of csRNA1-1. Analysis of the translational reporter fusion of PilT and an RNA-RNA mobility shift assay revealed direct binding of csRNA1-1 to *pilT* mRNA to control PilT expression. We also report the involvement of csRNAs in *S. sanguinis* biofilm formation.

RESULTS

Expression of csRNAs is regulated by CiaRH. To determine whether the expression of csRNAs is controlled by the CiaRH system in *S. sanguinis* ATCC 10556, we first constructed the following strains: wild-type (WT) ATCC 10556 containing an empty vector (WT mock), its *ciaRH* deletion mutant containing an empty vector (Δ *ciaRH* mock), and the complemented mutant derivative containing a plasmid-borne WT *ciaRH* allele (Δ *ciaRH*+pVACiaRH). Using these strains, real-time reverse transcription-PCR (RT-PCR) analysis of *csRNA* gene expression was performed. As shown in Table 1, transcription of all csRNAs, except for csRNA8, was almost completely lost in the Δ *ciaRH* strain, and the expression levels were restored in the Δ *ciaRH*+pVACiaRH complemented strain. These results confirm that the expression of csRNAs, except for csRNA8, is regulated by the CiaRH TCS in *S. sanguinis* ATCC 10556.

Computational prediction of csRNA targets. To identify genes that are controlled by csRNAs, we first searched the *S. sanguinis* SK36 genome with TargetRNA2 (25) using

csRNA sequences as queries. The complete lists of genes identified by these searches are shown in Tables S1 to S6 in the supplemental material. The number of predicted target genes of the csRNAs ranged from 10 to 57, with some overlap. The predicted target genes of csRNA1-1 and csRNA1-2 showed a high degree of overlap (31 shared genes out of 52 or 56 candidate target genes, respectively), which suggested that these two csRNAs share some regulatory functions. In addition, Marx et al. (20) have shown that the expression levels of csRNA1-1 and csRNA1-2 in *S. sanguinis* were significantly higher than those of other csRNAs by Northern blot analyses. Thus, csRNA1-1 and csRNA1-2 were selected for further functional analyses. A list of the top 10-ranked candidate target genes for csRNA1-1 and csRNA1-2 is shown in Table 2. Predicted targets included several putative surface protein genes, e.g., SSA_0227, SSA_1632, SSA_2121, SSA_0906, and SSA_0905 (Table 2 and Table S1), which suggests an important role of csRNA1-1 and csRNA1-2 in *S. sanguinis* colonization. Among the predicted targets, type IV pilus retraction ATPase gene *pilT* (SSA_2317) was the most probable target, with the lowest thermodynamic energy (-15.87 kcal/mol) of hybridization between the two RNA molecules. The *pilT* gene is a constituent of the type IV pilus gene cluster (26, 27). Type IV pili have been shown to mediate many functions in bacteria, including adherence to host cells, twitching motility, genetic competence, and biofilm formation (28, 29). Thus, we chose *pilT* as a target gene for further analyses of csRNA function in *S. sanguinis* ATCC 10556.

Expression of the *pilT* gene is negatively regulated by csRNA1-1 and csRNA1-2.

The *csRNA1-1* (90 bp in size) and *csRNA1-2* (94 bp in size) genes are tandemly located in the intergenic region between the *galM* (SSA_0062) and *ruvB* (SSA_0063) genes in the *S. sanguinis* SK36 genome (Fig. 1A) and have highly conserved nucleotide sequences (93% identity), suggesting they are gene duplications with similar physiological roles. Thus, to assess the physiological roles of csRNA1-1 and csRNA1-2, we generated a *csRNA1-1 csRNA1-2* double-deletion mutant strain via double-crossover recombination (Fig. 1A) and its derivative containing an empty vector ($\Delta csRNA1-1, 2$ mock). The complemented mutant derivative containing plasmid-borne WT *csRNA1-1* and *csRNA1-2* alleles ($\Delta csRNA1-1, 2 + pVA1-1, 2$) was also generated. Using these strains, we assessed whether the computationally identified target gene *pilT* is controlled by csRNA1-1 and csRNA1-2. As shown in Fig. 1B, real-time RT-PCR analyses revealed that the $\Delta csRNA1-1, 2$ strain contained about 2-fold increased levels of *pilT* mRNA, suggesting that csRNA1-1 and csRNA1-2 negatively regulate *pilT* mRNA levels. In addition, an approximately 10-fold reduction in *pilT* mRNA level was observed in the $\Delta csRNA1-1, 2 + pVA1-1, 2$ strain compared to the level in the WT strain. This reduction seemed to be the result of increased expression (about 5-fold compared to that of the parent strain) of *csRNA1-1* in the $\Delta csRNA1-1, 2 + pVA1-1, 2$ strain (Fig. 1C). This increase in *csRNA1-1* expression may be due to the increased copy number of the shuttle plasmid (pVA838) used for gene complementation. Using these strains, we also checked whether the other candidate target genes are controlled by csRNA1-1 and csRNA1-2. As shown in Fig. S1A, the level of SSA_2345 transcript (rank 2 in Table 2) was slightly decreased in the $\Delta csRNA1-1, 2$ mock strain, but the level was not changed in the $\Delta csRNA1-1, 2 + pVA1-1, 2$ strain. In contrast, the expression of SSA_2216 (*licD1*; rank 3 in Table 2) was significantly decreased in the $\Delta csRNA1-1, 2 + pVA1-1, 2$ strain but was not affected in the $\Delta csRNA1-1, 2$ mock strain (Fig. S1B). These results suggest that the mechanisms of gene regulation by csRNA1-1 and csRNA1-2 vary according to the target gene affected.

Expression of the *pilT* reporter gene is negatively regulated by csRNA1-1 and csRNA1-2. To confirm the results of real-time RT-PCR analyses shown in Fig. 1, we created a luciferase translational reporter strain (WT-luc) in which the structural gene of *pilT* is replaced with a luciferase gene (Fig. 2A). Using this strain, we further constructed the following strains: WT-luc containing an empty vector (WT-luc mock), a *csRNA1-1 csRNA1-2* double-deletion mutant containing an empty vector ($\Delta csRNA1-1, 2$ -luc mock), and the complemented mutant ($\Delta csRNA1-1, 2$ -luc + pVA1-1, 2). Luciferase assays using these strains indicated that the $\Delta csRNA1-1, 2$ -luc mock strain showed a significant

TABLE 2 Top 10-ranked putative target genes for csRNA1-1 and csRNA1-2

Rank ^a	Energy	Locus tag	Gene description (gene)	Putative interaction between targets and csRNA1-1 or csRNA1-2 ^b
1 (1)	-15.87	SSA_2317	Tfp pilus assembly protein, pilus retraction ATPase PilT	csRNA1-1 47 ACUUUUUCAAUCCUAA 31 ::: SSA_2317 -14 AGGGGAAGUUUAGGAUG 3
2 (2)	-14.36	SSA_2345	Hypothetical protein	csRNA1-1 60 ACCUCUAAUAAUACU 45 SSA_2345 -11 AGGGAGAUU-UUAUGU 4
3 (3)	-14.01	SSA_2216	Lipopolysaccharide biosynthesis protein (<i>licD1</i>)	csRNA1-1 52 UAAU-ACUUUUUCAAUCCUAA 32 : SSA_2216 -30 AUUAUUGAAAAGUUUGGGAG -10
4	-13.14	SSA_1763	Molybdenum ABC transporter ATPase	csRNA1-1 35 CCUAAUAGUUUGU 23 SSA_1763 8 AGAUUAUCAAACU 20
(4)	-13.19	SSA_1655	Hypothetical protein	csRNA1-2 23 UUCAAUCCUCC 13 SSA_1655 -78 CAGUUAGGAGA -68
5 (5)	-12.43	SSA_2217	Cps9H	csRNA1-1 48 UACUUUUUCAAUCCUAA 32 SSA_2217 -27 AUG-AAAAGUUUAGGAA -11
6 (6)	-11.89	SSA_1635	Hypothetical protein	csRNA1-1 62 CCUCUAAUAAUACUUUU 46 SSA_1635 2 GGAAAUUUAUUGAAAU 19
7 (7)	-11.64	SSA_0227	Collagen-binding surface protein	csRNA1-1 60 ACC-CUCUAAU-AAUACUUUU 42 : SSA_0227 -14 CGGAGGGAUUUUUAUG-AAA 6
8	-11.39	SSA_1820	Hypothetical protein	csRNA1-1 19 AAUCCCCG 11 SSA_1820 4 AUAGGGGA 12
37 (8)	-11.59	SSA_0718	Hypothetical protein	csRNA1-2 23 UUCAAUCCUCCAGA 10 : SSA_0718 -78 CAGUUAGGAAGUUA -65
9 (9)	-11.36	SSA_1632	Surface protein	csRNA1-1 59 CCCUCUAAUAAUACUU 44 SSA_1632 -11 AGGAGAUUAAAUG-A 4
10	-11.16	SSA_0991	DNase	csRNA1-1 51 UAAUACUUUUUCAAUCCU 33 SSA_0991 -3 UUUUUGAAAAGUUUAGGU 16
(10)	-11.35	SSA_2177	Hypothetical protein	csRNA1-2 51 ACUUUUUCAA-AUCCU 37 : SSA_1702 4 AGAAAAGUUACAGGG 19

^aRank for csRNA1-2 is indicated in parentheses.

^bVertical lines and dots between nucleotides of mRNA and csRNA indicate standard (Watson-Crick) and nonstandard (G-U wobble) base-pairing interactions, respectively.

increase in luciferase activity, and complementation of both csRNA1-1 and csRNA1-2 completely reversed the elevated luciferase activity (Fig. 2B). These results are consistent with the results of real-time RT-PCR analyses shown in Fig. 1. We next used complementation plasmids that contained the WT allele of *csRNA1-1* (pVA1-1) or *csRNA1-2* (pVA1-2) to construct strains that express only csRNA1-1 ($\Delta csRNA1-1$, 2-luc+pVA1-1) or csRNA1-2 ($\Delta csRNA1-1$, 2-luc+pVA1-2). We then performed a luciferase assay to determine the effect of csRNA1-1 and csRNA1-2 on PilT reporter activity. As shown in Fig. 2B, the $\Delta csRNA1-1$, 2-luc+pVA1-1 and $\Delta csRNA1-1$, 2-luc+pVA1-2 strains both showed

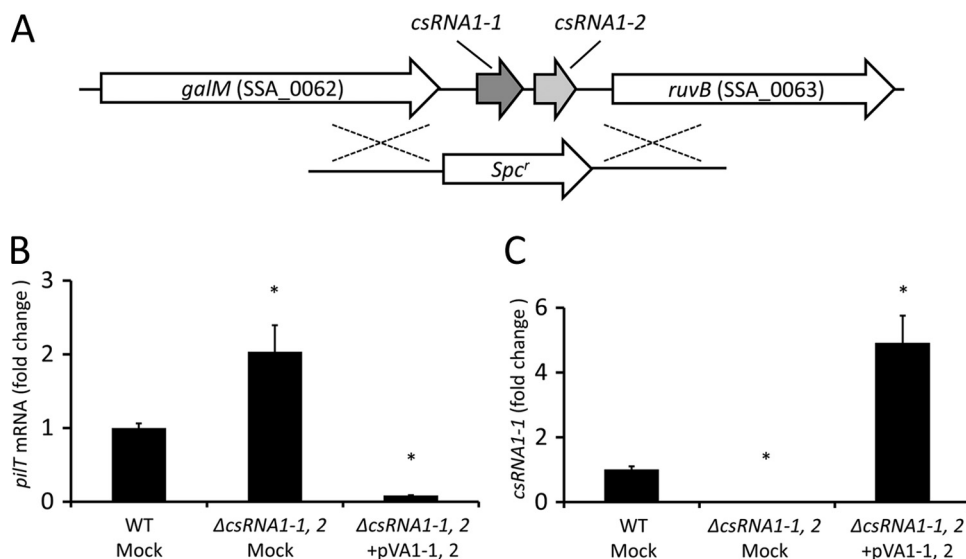


FIG 1 Regulation of *pilT* mRNA expression by *csRNA1-1* and *csRNA1-2*. (A) Schematic representation of *S. sanguinis* *csRNA1-1* and *csRNA1-2* genomic regions and the double-crossover event for generation of the *csRNA1-1 csRNA1-2* double-deletion mutant strain ($\Delta csRNA1-1, 2$). (B and C) Quantitative RT-PCR analysis of *pilT* (B) and *csRNA1-1* (C) expression in *S. sanguinis*. The $\Delta csRNA1-1, 2$ strain was transformed with either complementation plasmid pVA1-1, 2 or empty vector pVA838 (Mock). Strains were grown in BHI broth to the early exponential phase, and RNA was isolated and used in quantitative RT-PCR analysis. Data are expressed as means \pm standard deviations (SD) from triplicate experiments. *, $P < 0.01$.

luciferase activity comparable to that of the $\Delta csRNA1-1, 2$ -luc+pVA1-1, 2 strain, indicating that complementation with either *csRNA1-1* or *csRNA1-2* can sufficiently restore the inhibitory effect of *csRNA1-1* and *csRNA1-2* on PiT reporter activity. These results indicate that *csRNA1-1* and *csRNA1-2* have similar regulatory roles and can compensate for each other's functions, at least concerning the negative regulatory effect on PiT expression.

Time course of *pilT* gene expression. To assess whether *S. sanguinis pilT* gene expression varies according to growth phase, we measured the growth of the WT-luc

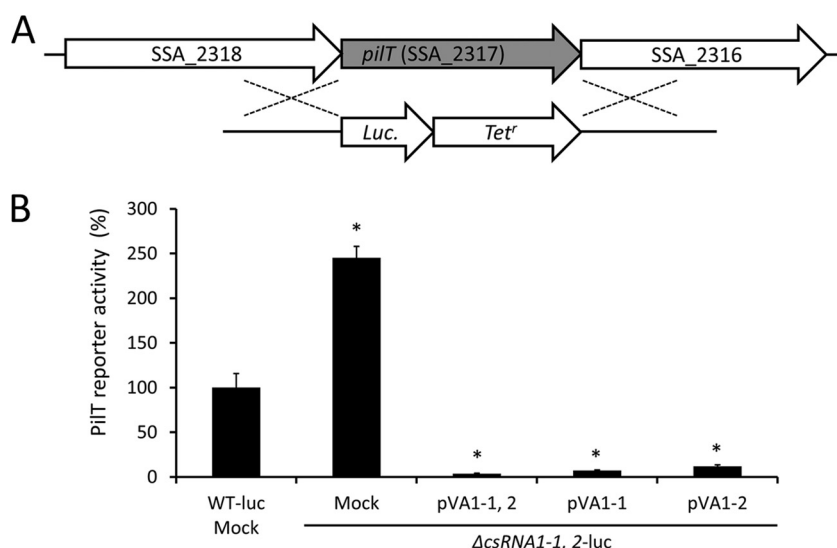


FIG 2 (A) Schematic representation of *S. sanguinis pilT* genomic regions and the double-crossover event for generation of PiT-luciferase translational reporter strain. (B) Regulation of translational luciferase fusion of *pilT* by *csRNA1-1* and *csRNA1-2*. PiT-luciferase reporter strains were grown in BHI broth to early exponential phase, and luciferase activity was measured. Data are normalized to the OD₆₀₀ of corresponding cultures and converted to percent luciferase activity relative to that of the WT-luc strain. Data are expressed as means \pm SD from triplicate experiments. *, $P < 0.01$.

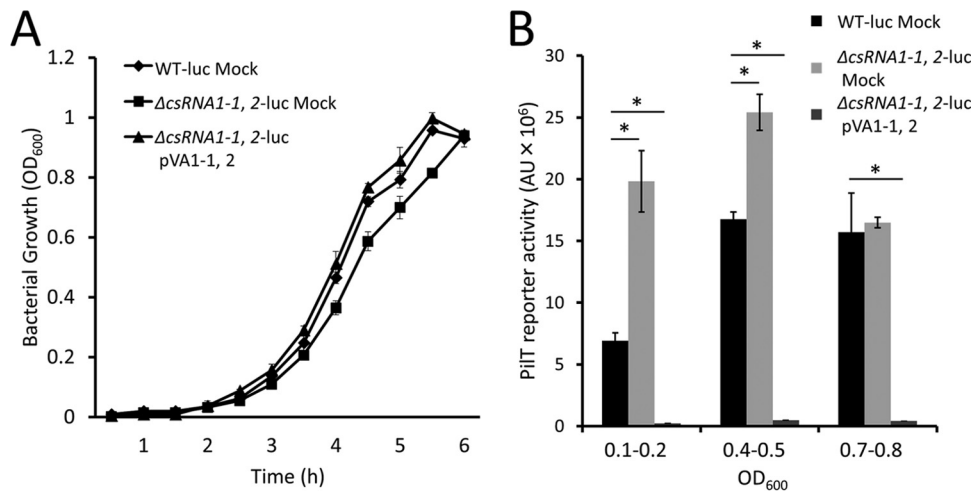


FIG 3 Growth phase-dependent expression of PiIT. PiIT-luciferase reporter strains were grown over a 6-h period, and samples were collected for luciferase assay at an OD₆₀₀ of 0.1 to 0.2 (early log phase), 0.4 to 0.5 (mid-log phase), and 0.7 to 0.8 (late-log phase). (A) Growth curves of the strains over the measurement period. (B) PiIT reporter activities of the strains. Luciferase activity was measured and divided by the OD₆₀₀ of corresponding cultures. Data are expressed as means \pm SD of arbitrary units (AU) from three independent cultures. *, $P < 0.01$.

mock, $\Delta csRNA1-1, 2$ -luc mock, and $\Delta csRNA1-1, 2$ -luc+pVA1-1, 2 strains over time (Fig. 3A). Luciferase activity of the strains then was measured at early log (optical density at 600 nm [OD₆₀₀] of 0.1 to 0.2), mid-log (0.4 to 0.5), and late log (0.7 to 0.8) phases (Fig. 3B). At early log phase, the luciferase activity of the $\Delta csRNA1-1, 2$ -luc mock strain was about three times higher than that of the WT-luc mock strain. The reporter activities increased to maximal levels at mid-log phase and decreased to similar levels at late-log phase. The PiIT reporter activity did not directly correlate with the *csRNA1-1* transcription level (Fig. S2) in the WT-luc mock strain, and growth phase-dependent changes in reporter activity were still observed in the $\Delta csRNA1-1, 2$ -luc mock strain, suggesting that PiIT expression is regulated by additional factors. In contrast to the $\Delta csRNA1-1, 2$ -luc mock strain, the PiIT reporter activity was scarcely detectable in the $\Delta csRNA1-1, 2$ -luc+pVA1-1, 2 strain throughout the growth phase. These results indicate that the observed difference in Fig. 2 is not caused by a difference in the timing of maximal expression of PiIT reporter activity.

A specific region of *csRNA1-1* is important for regulation of *piIT* gene expression. To confirm the importance of nucleotides in *csRNA1-1* predicted to base pair with *piIT* mRNA in the TargetRNA2 search (Fig. 4A), nucleotide substitution mutations (mut-1, mut-2, and mut-3) were introduced into the plasmid containing the *csRNA1-1* gene (pVA1-1) to obtain pVA1-1 mut-1, pVA1-1 mut-2, and pVA1-1 mut-3. These plasmids then were transformed into the $\Delta csRNA1-1, 2$ -luc mock strain, and the luciferase assay was performed to evaluate their ability to regulate PiIT expression. As shown in Fig. 4B, strains expressing mut-1 or mut-2 exhibited elevated levels of luciferase activity, similar to the $\Delta csRNA1-1, 2$ -luc mock strain, indicating that these mutants have lost their inhibitory effect on PiIT expression. In contrast, the strain expressing mut-3 retained *csRNA1-1* activity comparable to the WT level (Fig. 4B). The expression of all *csRNA1-1* versions used was confirmed by RT-PCR (Fig. 4C). Collectively, these results indicate that the AAAC sequence within *csRNA1-1*, which was mutated in both mut-1 and mut-2, is essential for the inhibitory effect of *csRNA1-1* on PiIT expression.

***csRNA1-1* directly binds to *piIT* mRNA.** To confirm whether *csRNA1-1* can bind directly to target mRNA to regulate its expression, we performed an RNA-RNA electrophoretic mobility shift assay (EMSA) using *csRNA1-1* and *piIT* mRNA. To show the specificity of RNA-RNA interaction, the mutant version of *csRNA1-1* (mut-2 in Fig. 4) and the *piIT* mRNA mutant (mut) with the respective compensatory nucleotide substitutions

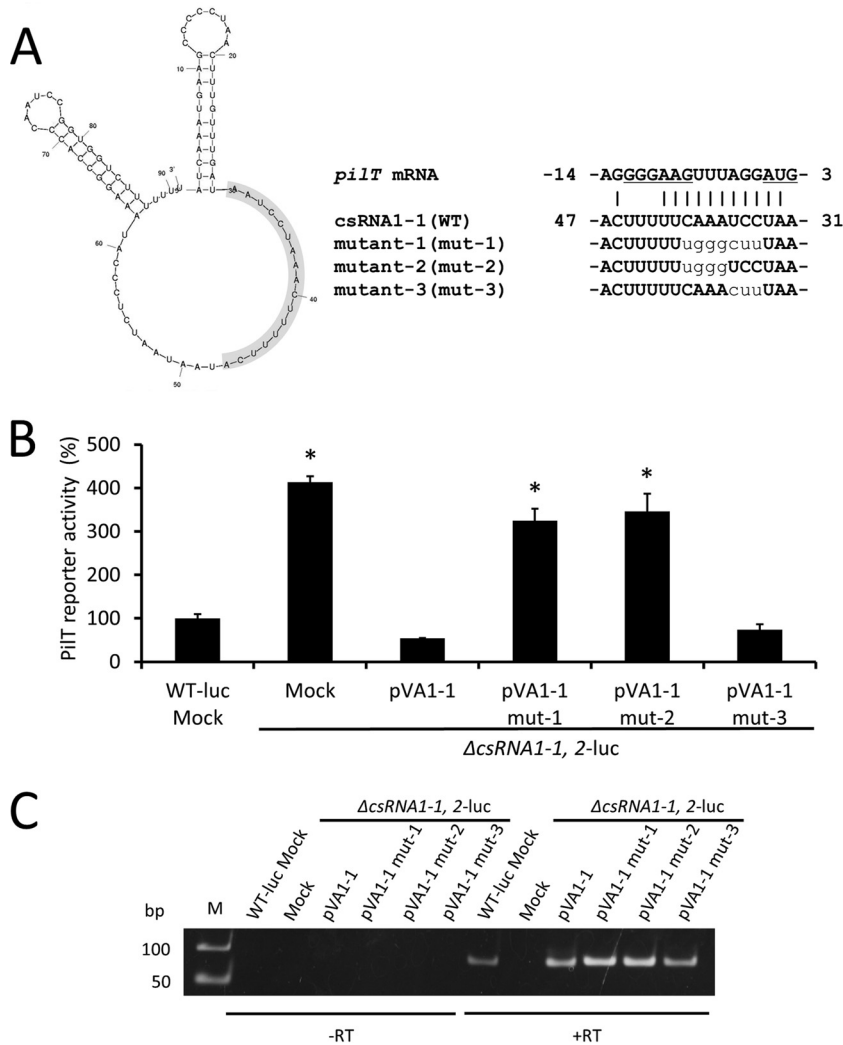


FIG 4 Effect of csRNA1-1 mutation on PiIT expression. (A, left) Putative secondary structure of csRNA1-1, as predicted by Mfold (41). The nucleotides involved in the putative region for hybridization with *piIT* mRNA are highlighted in gray background. (Right) Putative interactions between the 5' end of *piIT* mRNA and csRNA1-1 WT or mutant strains (mut-1, mut-2, and mut-3). The ribosome binding site and start codon are underlined. Substituted nucleotides in csRNA1-1 mutants are shown in plain lowercase. (B) Luciferase activity of *S. sanguinis* csRNA1-1 mutant strains (mut-1, mut-2, and mut-3). Strains were grown in BHI broth to early exponential phase and luciferase activity was measured. Data are presented as percent luciferase activity relative to that of the WT-luc strain. Data are expressed as means \pm SD from triplicate experiments. *, $P < 0.01$. (C) RT-PCR analysis of *csRNA1-1* expression in *S. sanguinis* csRNA1-1 mutant strains. Strains were grown to early exponential phase, and RNA was isolated and used in RT-PCR analysis. The image shown is representative of three independent experiments.

were also used. Putative interactions between *piIT* mRNA (WT) and csRNA1-1 (WT) or *piIT* mRNA (mut) and csRNA1-1 (mut-2) are shown in Fig. 5A. Incubation of *in vitro*-transcribed *piIT* mRNA (WT) with digoxigenin (DIG)-labeled csRNA1-1 (WT) resulted in the emergence of a higher-molecular-weight complex, and the band intensity decreased significantly when DIG-labeled csRNA1-1 (mut-2) was used as the probe ($P < 0.01$) (Fig. 5B and C, lanes 5 and 6). In contrast, incubation of *piIT* mRNA (mut) with DIG-labeled csRNA1-1 (WT) resulted in a faint band, and a significantly higher-intensity band was observed after incubation with csRNA1-1 (mut-2) ($P < 0.01$) (Fig. 5B and C, lanes 7 and 8). An approximately 2-fold increase in the intensity of the shifted band was observed in lane 8 compared with lane 5 (Fig. 5B and C). This difference may be caused by the increased GC content within the putative

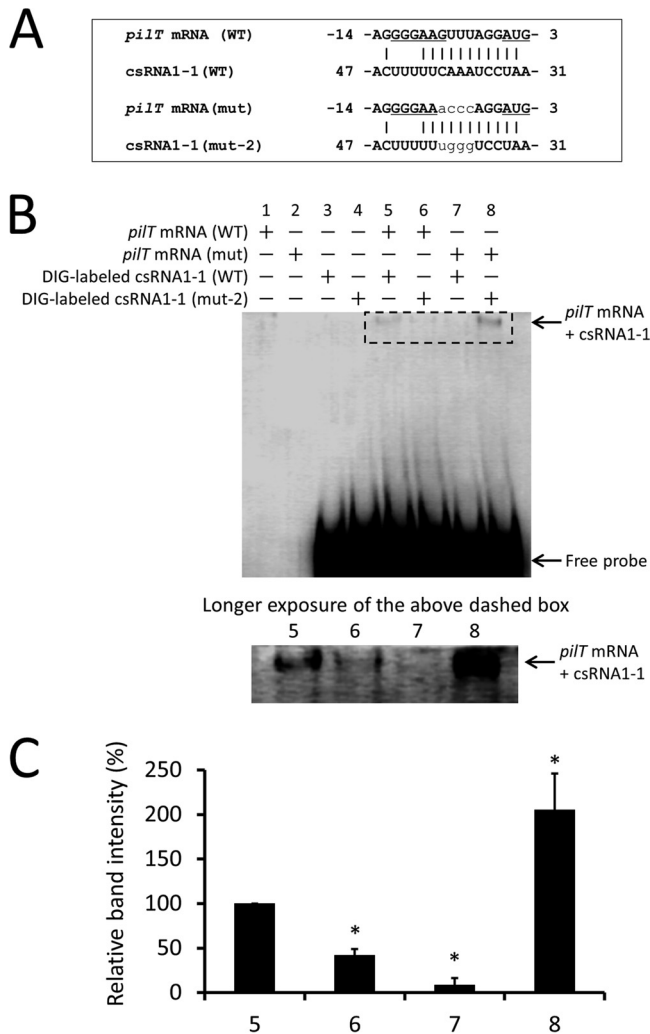


FIG 5 RNA-RNA electrophoretic mobility shift assay of csRNA1-1 with *pilT* mRNA. (A) Putative interactions between the 5' end of *pilT* mRNA (WT) and csRNA1-1 (WT) or *pilT* mRNA (mut) and csRNA1-1 (mut-2). The ribosome binding site and start codon are underlined. Substituted nucleotides in mutants are shown in plain lowercase. (B) DIG-labeled csRNA1-1 WT or csRNA1-1 mut-2 was incubated with *pilT* mRNA (WT) or *pilT* mRNA mutant (mut). Reaction products were separated on 5% native polyacrylamide gel and transferred to a membrane. DIG-labeled RNA signals on the membrane were detected using anti-DIG antibody. The image shown is representative of three independent experiments. The shifted bands in lanes 5 to 8 (the region surrounded by a dashed-line rectangle) are shown with a longer exposure time in the lower panel. (C) Quantification of the intensity of shifted bands in lanes 5 to 8. Data are expressed as means \pm SD from three independent experiments. *, $P < 0.01$.

binding region of *pilT* mRNA (mut) and csRNA1-1 (mut-2) (Fig. 5A). These results clearly indicate that csRNA1-1 directly binds to *pilT* mRNA, and the AAAC sequence within csRNA1-1 is important for the binding. In addition, together with the results shown in Fig. 4, the inhibitory effect of csRNA1-1 on PilT expression appears to be dependent on its ability to bind *pilT* mRNA.

csRNA1-1 and csRNA1-2 inhibit biofilm formation in *S. sanguinis*. Type IV pili are known to mediate attachment and colonization of various surfaces (29). In addition, some of the predicted target genes of csRNA1-1 (Table 2), such as SSA_0227, SSA_1632, SSA_2121, SSA_0906, and SSA_0905, are putative surface proteins that may be involved in *S. sanguinis* biofilm formation. Thus, we hypothesized that csRNA1-1 and csRNA1-2 play a regulatory role in *S. sanguinis* biofilm formation. To test this hypothesis, we performed biofilm formation assays using WT mock, Δ csRNA1-1, 2 mock, and Δ csRNA1-1, 2+pVA1-1, 2 strains. As shown in Fig. 6, the Δ csRNA1-1, 2 mock strain showed a significant increase in

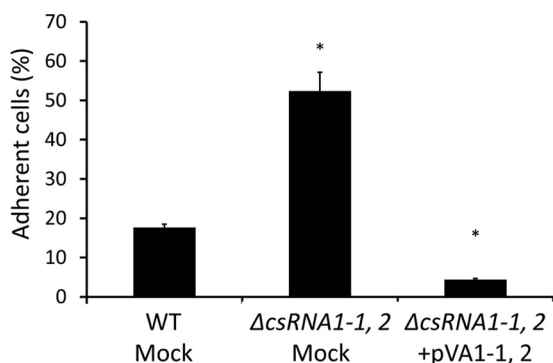


FIG 6 Effect of csRNA1-1 and csRNA1-2 deletion on biofilm formation. *S. sanguinis* strains were grown in BHI broth containing 1% sucrose on saliva-coated 24-well polystyrene plates. Adherent and nonadherent cells were separately collected and quantified by measuring OD₆₂₀. Percentages of adherent cells were calculated by the following equation: $100 \times \text{OD}_{620}$ of adherent cells / OD_{620} of total (adherent and nonadherent) cells. *, $P < 0.01$.

biofilm formation compared with the WT mock strain, and this increase was reversed in the $\Delta csRNA1-1, 2$ +pVA1-1, 2 strain. On the basis of these results, csRNA1-1 and csRNA1-2 appear to play inhibitory roles in *S. sanguinis* biofilm formation.

DISCUSSION

Bacterial gene regulation by sRNAs has attracted increasing attention in recent years because sRNAs are implicated in many biological processes, including environmental adaptation and pathogenesis. In streptococci, a substantial number of sRNAs, mainly from the two major human pathogens *S. pyogenes* and *S. pneumoniae*, have been predicted through computational approaches or experimentally identified using next-generation sequencing (RNA-seq) (30, 31). However, only a few of these sRNAs have known functions thus far. csRNAs of *S. pneumoniae* are a well-studied example of streptococcal sRNAs, which are involved in competence control (32, 33, 34). Because the CiaRH TCS is conserved in all streptococci and controls a variety of physiological processes, including environmental stress tolerance, it is conceivable that csRNAs play important roles in the physiology of streptococci. Using a target prediction program (TargetRNA2), we searched for genes that are regulated by csRNA1-1 and csRNA1-2 in the *S. sanguinis* genome. Among various candidate target genes, *pilT*, a constituent of the type IV pilus gene cluster, was the most probable target, and indeed *pilT* gene expression was shown to be negatively regulated by csRNA1-1 and csRNA1-2 in *S. sanguinis* (Fig. 1 and 2).

Type IV pili are surface-exposed filaments that promote properties such as adhesion, protein secretion, DNA uptake, and motility (29). Although type IV pili have been studied extensively in a few Gram-negative species, including *Pseudomonas* and *Neisseria*, little is known about type IV pili of Gram-positive species, including streptococci. It is only recently that the functional analysis of type IV pili in *S. sanguinis* has been reported (27). The 22-kb-long type IV pilus gene cluster of *S. sanguinis* is conserved in almost all *S. sanguinis* strains and absent from all other streptococcal species (27). This species-specific conservation of the gene cluster raises the possibility that type IV pili play important roles in the physiology of *S. sanguinis*.

Twisting motility is a form of solid-surface translocation that occurs in a wide range of bacteria (35). The movement is mediated by type IV pilus retraction, which is powered by the ATPase PilT (36). Twisting motility has been observed in a limited number of *S. sanguinis* strains other than SK36 or ATCC 10556 (27). We first hypothesized that the twisting motility-negative phenotype of *S. sanguinis* strains such as SK36 and ATCC 10556 is a consequence of a negative regulatory effect of csRNA1-1 and csRNA1-2 on PilT expression. However, we did not observe twisting motility in either the ATCC 10556 WT or $\Delta csRNA1-1, 2$ strain (data not shown). Because twisting motility

can be influenced by many factors, including substrate topography, fluidity, stiffness, surface coating, secretion of biological molecules, and oxygen levels (37), it is possible that under some currently unknown physiological conditions, twitching motility-negative strains such as SK36 and ATCC 10556 can exhibit twitching motility.

csRNAs show a high degree of similarity to each other, particularly in the unpaired region between the two stem-loop structures. Complementarity to the ribosome binding site and the AUG start codon within this unpaired region has been suggested to allow csRNA to bind to target mRNA and inhibit translational initiation (20). Consistent with these predictions, we showed that csRNA1-1 binds directly to its target, *pilT* mRNA, in RNA-RNA EMSA (Fig. 5). To our knowledge, this is the first experimental observation of direct binding between a csRNA and a target mRNA. The nucleotide sequence that was important for base pairing with *pilT* mRNA, which resided in proximity of the ribosome binding site and AUG (Fig. 4), was not identical to the previously defined complementary sequence to the start codon and ribosome binding site (20). This discrepancy suggests the diversity of mechanisms by which csRNAs control target mRNA expression.

Biofilm formation by *S. sanguinis* is a complex process involving many factors, such as adhesins, signaling systems, glucosyltransferases, and extracellular DNA (1, 2, 4, 38, 39). In our *in vitro* biofilm assay using sucrose-containing medium, a saliva coating on culture plates was also essential for biofilm formation of *S. sanguinis* WT and mutant strains, because all strains tested formed almost no biofilm on uncoated plates (data not shown). In addition, the inhibitory effect of csRNA1-1 and csRNA1-2 on biofilm formation was observed only in cultures grown under gentle agitation (Fig. 6). No inhibitory effect was observed with static culture, in which all *S. sanguinis* strains tested readily formed biofilms and showed no significant difference in biofilm-forming ability (data not shown). In static culture, *S. sanguinis* cells that have settled to the bottom of the well can synthesize water-soluble glucan and may adhere to the polystyrene surface regardless of the presence or absence of initial attachment. Conversely, during culture with agitation, in which *S. sanguinis* cannot readily settle to the bottom of the well, initial attachment to saliva-coated surfaces with adhesins may be essential for biofilm formation. Thus, the observed difference between *S. sanguinis* WT and $\Delta csRNA1-1, 2$ strains in biofilm formation with agitated culture seemed to be caused by the difference in the ability of initial attachment.

Although *S. sanguinis* SK36 has pili that contribute to cell adhesion and biofilm formation (38, 40), strain ATCC 10556 does not express pili (40). It has not been assessed whether type IV pili of *S. sanguinis* contribute to initial attachment; however, it is conceivable that increased PilT expression in the $\Delta csRNA1-1, 2$ strain contributed, at least in part, to elevated biofilm formation in this strain. In addition, although we did not assess the expression of other putative adhesin genes in the $\Delta csRNA1-1, 2$ strain, it is possible that the regulation of these genes by csRNA1-1 and csRNA1-2 also could affect biofilm-forming ability. Although extracellular signals that are sensed by the CiaRH system in *S. sanguinis* are yet to be determined, the regulation of PilT expression by csRNA1-1 and csRNA1-2 provides new insight into molecular mechanisms underlying csRNA-mediated regulation in *S. sanguinis* colonization.

MATERIALS AND METHODS

Bacterial strains and growth conditions. *S. sanguinis* strains used in this study are listed in Table S7 in the supplemental material. Strains were routinely grown in brain heart infusion (BHI) broth (BD) at 37°C under anaerobic conditions (10% H₂, 10% CO₂, and 80% N₂). For antibiotic selection, 250 µg/ml of spectinomycin (Spec), 12.5 µg/ml of tetracycline (Tet), or 5 µg/ml of erythromycin was used. *Escherichia coli* strain DH5α was aerobically grown in Lennox L broth (Invitrogen), and 100 µg/ml of ampicillin or 17 µg/ml of chloramphenicol was used for antibiotic selection. Transformation of *S. sanguinis* strains was performed as described previously (21), with some modifications. Briefly, cultures in 3 ml of Todd-Hewitt (TH) broth (Difco) adjusted to pH 7.6 were incubated at 37°C overnight under anaerobic conditions. One microliter of each culture was transferred to 5 ml of TH broth (pH 7.6) containing 10% horse serum and statically incubated at 37°C under aerobic conditions for 2 h. After incubation, aliquots of the cultures were mixed with transforming DNA (1 µg/ml) in a 1.5-ml microtube and further incubated for 5 h. The cells then were plated on BHI agar containing appropriate antibiotics and grown under anaerobic conditions at 37°C for 48 h.

Construction of *S. sanguinis* mutant and complemented strains. The *csRNA1-1 csRNA1-2* double-deletion mutant and *ciaRH* deletion mutant strains of *S. sanguinis* were created by replacement of the target genes with a Spec resistance cassette (Sp^r). Sp^r was cloned into the BamHI site of pUC18 to obtain pUC18 Sp^r. The upstream and downstream fragments of the target genes (400 to 500 bp in size) were cloned into pUC18 Sp^r at sites SphI/SalI and SmaI/EcoRI, respectively, using primers listed in Table S8. The obtained plasmids were linearized with EcoRI digestion and transformed into *S. sanguinis* ATCC 10556, and deletion of the target genes was confirmed by PCR. For complementation studies, wild-type (WT) *csRNA1-1* and/or *csRNA1-2* or *ciaRH* alleles were cloned into the *E. coli*-streptococci shuttle vector pVA838 (22) via Sall/SphI sites for *csRNA1-1* and *csRNA1-2* or Sall site for *ciaRH* to obtain pVA1-1, 2, pVA1-1, pVA1-2, and pVAciARH plasmids, respectively. These plasmids were transformed into the respective mutant strains, and genetic complementation of the genes was confirmed by real-time PCR.

RNA isolation and quantitative RT-PCR. *S. sanguinis* cultures were grown to early exponential phase (OD₆₀₀ of 0.1 to 0.2), and RNA was isolated from cells subjected to bead beating using the RNeasy minikit (Qiagen) and treated with Turbo DNase (Ambion). cDNA was synthesized from RNA using the ReverTra Ace quantitative PCR RT kit (Toyobo) according to the manufacturer's instructions. Quantitative PCR was performed using the StepOnePlus real-time PCR system (Life Technology) with Fast SYBR green master mix (Thermo Fisher). Primers used in the experiments are listed in Table S8. Results were normalized to *S. sanguinis* 16S rRNA gene expression. Experiments were performed in triplicate with at least three independent RNA samples.

Construction of plasmid-borne mutant *csRNA1-1* alleles. Nucleotide substitution mutants of plasmid-borne *csRNA1-1* were constructed with the QuikChange II site-directed mutagenesis kit (Agilent) according to the manufacturer's instructions, with slight modifications. The pVA1-1 plasmid, which contains the WT allele of *csRNA1-1*, and primers containing the desired mutation (listed in Table S8) were used for PCR amplification. After PCR, template DNA was digested with DpnI, and the resultant reaction product containing mutant plasmid was transformed into *E. coli* DH5 α cells. The generation of mutations was confirmed by DNA sequencing. The obtained plasmids that contained the desired mutations are designated pVA1-1 mut-1, pVA1-1 mut-2, and pVA1-1 mut-3, respectively.

Construction of PiIT-luciferase reporter strain and luciferase assay. A single-copy reporter fusion of *piIT* in the native chromosomal context was generated as follows. The Tet resistance cassette (Tet^r) was cloned into pUC18 at the BamHI site to obtain pUC18 Tet^r. Using the two-step overlap PCR method (23), the upstream region of *piIT* was fused to the open reading frame of the luciferase gene *NanoLuc*, amplified from the pNL1.1 vector (Promega), and cloned into pUC18 Tet^r at SphI/SalI sites. The downstream PCR fragment of the *piIT* gene then was cloned into SmaI/EcoRI sites, resulting in generation of the *piIT*-NanoLuc-Tet^r fusion plasmid, which was linearized with EcoRI digestion and transformed into *S. sanguinis* ATCC 10556. A schematic illustration of the double-crossover event is shown in Fig. 2A. The obtained PiIT-luciferase reporter strain, which has the promoterless luciferase gene replaced with the *piIT* gene in the chromosome, is designated WT-luc. Using WT-luc as a parent strain, *csRNA1-1* and *csRNA1-2* deletion mutants and complemented strains were also generated (Table S7). The luciferase assay was performed using the Nano-Glo Dual-Luciferase reporter assay kit (Promega) according to the manufacturer's instructions, with some modifications. Briefly, *S. sanguinis* luc strains were grown in BHI broth to early exponential phase (OD₆₀₀ of 0.1 to 0.2). Subsequently, 50 μ l of the culture was transferred to a 96-well plate, and 25 μ l of NanoDLR Stop and Glo reagent (Promega) was added to the wells. After incubation at room temperature for 10 min, luminescence was measured with the GloMax-Multi detection system (Promega). Relative luminescence units were normalized to the OD₆₀₀ of corresponding cultures. Experiments were performed in triplicate with at least three independent cultures.

In vitro transcription reactions. *In vitro*-transcribed RNAs for use in the RNA-RNA electrophoretic mobility shift assay (EMSA) were created using the CUGA7 *in vitro* transcription kit (Nippon Gene), and digoxigenin (DIG)-labeled *csRNA1-1* and *csRNA1-1* mut-2, which were used as RNA probes, were synthesized using the DIG Northern Starter kit (Roche) according to the manufacturer's instructions. Template DNA for *piIT* mRNA (WT) and *piIT* mRNA (mut) or *csRNA1-1* transcription was PCR amplified or chemically synthesized, respectively. The T7 promoter sequence was fused to the 5' end of DNA templates to allow transcription using T7 RNA polymerase. The primers used are listed in Table S8. After the transcription reaction, template DNA was removed by DNase treatment, and RNA products were purified with the RNA Clean & Concentrator kit (Zymo Research).

RNA-RNA EMSA. Direct interaction between *csRNA1-1* and *piIT* mRNA was examined by RNA-RNA EMSA analysis as described previously (24), with some modifications. RNAs were heated at 90°C for 2 min in 10 mM Tris-HCl (pH 7.5), 50 mM NaCl, 50 mM KCl, 0.5 mM EDTA, and 10% glycerol. RNAs then were cooled on ice for 5 min to allow them to fold. After the folding reaction, the DIG-labeled RNA probe, *csRNA1-1* WT or *csRNA1-1* mut-2 (15 ng each), and *piIT* mRNA (WT) or *piIT* mRNA (mut) (500 ng each) were mixed and incubated at 37°C for 15 min. The reaction products were then separated on 5% native polyacrylamide gel in 1 \times Tris-borate-EDTA buffer and electrically transferred onto a Hybond N+ membrane (GE). After UV cross-linking, DIG-labeled RNA signals on the membrane were detected using an alkaline phosphatase-conjugated anti-DIG antibody with CSPD-Star detection reagent (Roche) according to the manufacturer's instructions. The signal intensity for each band was quantified using LI-COR Image Studio software.

Biofilm formation assay. Overnight cultures of *S. sanguinis* strains were diluted 1:100 into fresh BHI broth containing 1% sucrose, transferred (500 μ l/well) to a 24-well polystyrene plate (Iwaki) coated with saliva, and incubated anaerobically at 37°C with rotary agitation at 80 rpm for 24 h. After incubation, culture medium containing nonadherent cells was transferred to a 1.5-ml microtube and the cells were collected by centrifugation (12,000 \times g, 5 min). The precipitated cells then were suspended with 200 μ l of 0.1 M NaOH. Adherent cells were detached and suspended by adding 200 μ l of 0.1 M NaOH to the wells. The suspensions of

adherent or nonadherent cells were transferred to a 96-well plate and quantified by measuring the OD₆₂₀ with a microplate reader (Tecan). The percentages of adherent cells were calculated by the following equation: $100 \times \text{OD}_{620} \text{ of adherent cells} / \text{OD}_{620} \text{ of total (adherent and nonadherent) cells}$.

Statistical analysis. The statistical significance of data obtained from quantitative RT-PCR, luciferase assay, and biofilm formation assay was determined by Student's *t* tests. *P* values of <0.01 were considered statistically significant.

SUPPLEMENTAL MATERIAL

Supplemental material for this article may be found at <https://doi.org/10.1128/IAI.00894-17>.

SUPPLEMENTAL FILE 1, PDF file, 0.7 MB.

ACKNOWLEDGMENTS

We thank Christina Croney from Edanz Group for editing a draft of the manuscript.

This work was supported in part by JSPS KAKENHI grant number JP17K11627. The funders had no role in study design, data collection and interpretation, or the decision to submit the work for publication.

C.O., H.M., M.N., N.O., and H. Kuwata designed the study. C.O. and H.M. performed experiments and wrote the initial draft of the manuscript. T.A., H.F., H. Kataoka, and H. Kuwata contributed to analysis and interpretation of data and assisted in the preparation of the manuscript. All other authors contributed to data collection and interpretation and critically reviewed the manuscript. All authors approved the final version of the manuscript and agree to be accountable for all aspects of the work in ensuring that questions related to the accuracy or integrity of any part of the work are appropriately investigated and resolved.

We have no conflicts of interest to declare.

REFERENCES

- Gong K, Mailloux L, Herzberg MC. 2000. Salivary film expresses a complex, macromolecular binding site for *Streptococcus sanguis*. *J Biol Chem* 275:8970–8974. <https://doi.org/10.1074/jbc.275.12.8970>.
- Tamesada M, Kawabata S, Fujiwara T, Hamada S. 2004. Synergistic effects of streptococcal glucosyltransferases on adhesive biofilm formation. *J Dent Res* 83:874–879. <https://doi.org/10.1177/154405910408301110>.
- Kreth J, Merritt J, Shi W, Qi F. 2005. Competition and coexistence between *Streptococcus mutans* and *Streptococcus sanguinis* in the dental biofilm. *J Bacteriol* 187:7193–7203. <https://doi.org/10.1128/JB.187.21.7193-7203.2005>.
- Kreth J, Vu H, Zhang Y, Herzberg MC. 2009. Characterization of hydrogen peroxide-induced DNA release by *Streptococcus sanguinis* and *Streptococcus gordonii*. *J Bacteriol* 191:6281–6291. <https://doi.org/10.1128/JB.00906-09>.
- Wagner EG, Romby P. 2015. Small RNAs in bacteria and archaea: who they are, what they do, and how they do it. *Adv Genet* 90:133–208.
- Miller EW, Cao TN, Pflughoeft KJ, Sumbly P. 2014. RNA-mediated regulation in Gram-positive pathogens: an overview punctuated with examples from the group A *Streptococcus*. *Mol Microbiol* 94:9–20. <https://doi.org/10.1111/mmi.12742>.
- Brantl S, Brückner R. 2014. Small regulatory RNAs from low-GC Gram-positive bacteria. *RNA Biol* 11:443–456. <https://doi.org/10.4161/ma.28036>.
- Kreikemeyer B, Boyle MD, Buttaro BA, Heinemann M, Podbielski A. 2001. Group A streptococcal growth phase-associated virulence factor regulation by a novel operon (Fas) with homologies to two-component-type regulators requires a small RNA molecule. *Mol Microbiol* 39:392–406. <https://doi.org/10.1046/j.1365-2958.2001.02226.x>.
- Ramirez-Peña E, Treviño J, Liu Z, Perez N, Sumbly P. 2010. The group A *Streptococcus* small regulatory RNA FasX enhances streptokinase activity by increasing the stability of the *ska* mRNA transcript. *Mol Microbiol* 78:1332–1347. <https://doi.org/10.1111/j.1365-2958.2010.07427.x>.
- Liu Z, Treviño J, Ramirez-Peña E, Sumbly P. 2012. The small regulatory RNA FasX controls pilus expression and adherence in the human bacterial pathogen group A *Streptococcus*. *Mol Microbiol* 86:140–154. <https://doi.org/10.1111/j.1365-2958.2012.08178.x>.
- Danger JL, Makthal N, Kumaraswami M, Sumbly P. 2015. The FasX small regulatory RNA negatively regulates the expression of two fibronectin-binding proteins in group A *Streptococcus*. *J Bacteriol* 197:3720–3730. <https://doi.org/10.1128/JB.00530-15>.
- Mascher T, Helmmann JD, Uden G. 2006. Stimulus perception in bacterial signal-transducing histidine kinases. *Microbiol Mol Biol Rev* 70:910–938. <https://doi.org/10.1128/MMBR.00020-06>.
- West AH, Stock AM. 2001. Histidine kinases and response regulator proteins in two-component signaling systems. *Trends Biochem Sci* 26:369–376. [https://doi.org/10.1016/S0968-0004\(01\)01852-7](https://doi.org/10.1016/S0968-0004(01)01852-7).
- Guenzi E, Gasc AM, Sicard MA, Hakenbeck R. 1994. A two-component signal-transducing system is involved in competence and penicillin susceptibility in laboratory mutants of *Streptococcus pneumoniae*. *Mol Microbiol* 12:505–515. <https://doi.org/10.1111/j.1365-2958.1994.tb01038.x>.
- Giammarinaro P, Sicard M, Gasc AM. 1999. Genetic and physiological studies of the CiaH-CiaR two-component signal-transducing system involved in cefotaxime resistance and competence of *Streptococcus pneumoniae*. *Microbiology* 145(Part 8):1859–1869.
- Sebert ME, Palmer LM, Rosenberg M, Weiser JN. 2002. Microarray-based identification of *htrA*, a *Streptococcus pneumoniae* gene that is regulated by the CiaRH two-component system and contributes to nasopharyngeal colonization. *Infect Immun* 70:4059–4067. <https://doi.org/10.1128/IAI.70.8.4059-4067.2002>.
- Dawid S, Sebert ME, Weiser JN. 2009. Bacteriocin activity of *Streptococcus pneumoniae* is controlled by the serine protease HtrA via posttranscriptional regulation. *J Bacteriol* 191:1509–1518. <https://doi.org/10.1128/JB.01213-08>.
- Ibrahim YM, Kerr AR, McCluskey J, Mitchell TJ. 2004. Control of virulence by the two-component system CiaR/H is mediated via HtrA, a major virulence factor of *Streptococcus pneumoniae*. *J Bacteriol* 186:5258–5266. <https://doi.org/10.1128/JB.186.16.5258-5266.2004>.
- Halfmann A, Kovács M, Hakenbeck R, Brückner R. 2007. Identification of the genes directly controlled by the response regulator CiaR in *Streptococcus pneumoniae*: five out of 15 promoters drive expression of small non-coding RNAs. *Mol Microbiol* 66:110–126. <https://doi.org/10.1111/j.1365-2958.2007.05900.x>.
- Marx P, Nuhn M, Kovács M, Hakenbeck R, Brückner R. 2010. Identification of genes for small non-coding RNAs that belong to the regulon of the

- two-component regulatory system CiaRH in *Streptococcus*. BMC Genomics 11:661. <https://doi.org/10.1186/1471-2164-11-661>.
21. Paik S, Senty L, Das S, Noe JC, Munro CL, Kitten T. 2005. Identification of virulence determinants for endocarditis in *Streptococcus sanguinis* by signature-tagged mutagenesis. Infect Immun 73:6064–6074. <https://doi.org/10.1128/IAI.73.9.6064-6074.2005>.
 22. Macrina FL, Tobian JA, Jones KR, Evans RP, Clewell DB. 1982. A cloning vector able to replicate in *Escherichia coli* and *Streptococcus sanguis*. Gene 19:345–353. [https://doi.org/10.1016/0378-1119\(82\)90025-7](https://doi.org/10.1016/0378-1119(82)90025-7).
 23. Kuwayama H, Obara S, Morio T, Katoh M, Urushihara H, Tanaka Y. 2002. PCR-mediated generation of a gene disruption construct without the use of DNA ligase and plasmid vectors. Nucleic Acids Res 30:E2. <https://doi.org/10.1093/nar/30.2.e2>.
 24. Henderson CA, Vincent HA, Stone CM, Phillips JO, Cary PD, Gowers DM, Callaghan AJ. 2013. Characterization of MicA interactions suggests a potential novel means of gene regulation by small non-coding RNAs. Nucleic Acids Res 41:3386–3397. <https://doi.org/10.1093/nar/gkt008>.
 25. Kery MB, Feldman M, Livny J, Tjaden B. 2014. TargetRNA2: identifying targets of small regulatory RNAs in bacteria. Nucleic Acids Res 42:W124–W129. <https://doi.org/10.1093/nar/gku317>.
 26. Xu P, Alves JM, Kitten T, Brown A, Chen Z, Ozaki LS, Manque P, Ge X, Serrano MG, Puiu D, Hendricks S, Wang Y, Chaplin MD, Akan D, Paik S, Peterson DL, Macrina FL, Buck GA. 2007. Genome of the opportunistic pathogen *Streptococcus sanguinis*. J Bacteriol 189:3166–3175. <https://doi.org/10.1128/JB.01808-06>.
 27. Gurung I, Spielman I, Davies MR, Lala R, Gaustad P, Biais N, Pelicic V. 2016. Functional analysis of an unusual type IV pilus in the Gram-positive *Streptococcus sanguinis*. Mol Microbiol 99:380–392. <https://doi.org/10.1111/mmi.13237>.
 28. Melville S, Craig L. 2013. Type IV pili in Gram-positive bacteria. Microbiol Mol Biol Rev 77:323–341. <https://doi.org/10.1128/MMBR.00063-12>.
 29. Berry JL, Pelicic V. 2015. Exceptionally widespread nanomachines composed of type IV pilins: the prokaryotic Swiss Army knives. FEMS Microbiol Rev 39:134–154. <https://doi.org/10.1093/femsre/fuu001>.
 30. Le Rhun A, Charpentier E. 2012. Small RNAs in streptococci. RNA Biol 9:414–426. <https://doi.org/10.4161/rna.20104>.
 31. Patenge N, Pappesch R, Khani A, Kreikemeyer B. 2015. Genome-wide analyses of small non-coding RNAs in streptococci. Front Genet 6:189.
 32. Tsui HC, Mukherjee D, Ray VA, Sham LT, Feig AL, Winkler ME. 2010. Identification and characterization of noncoding small RNAs in *Streptococcus pneumoniae* serotype 2 strain D39. J Bacteriol 192:264–279. <https://doi.org/10.1128/JB.01204-09>.
 33. Laux A, Sexauer A, Sivaselvarajah D, Kaysen A, Brückner R. 2015. Control of competence by related non-coding csRNAs in *Streptococcus pneumoniae* R6. Front Genet 6:246.
 34. Schnorpfel A, Kranz M, Kovács M, Kirsch C, Gartmann J, Brunner I, Bittmann S, Brückner R. 2013. Target evaluation of the non-coding csRNAs reveals a link of the two-component regulatory system CiaRH to competence control in *Streptococcus pneumoniae* R6. Mol Microbiol 89:334–349. <https://doi.org/10.1111/mmi.12277>.
 35. Mattick JS. 2002. Type IV pili and twitching motility. Annu Rev Microbiol 56:289–314. <https://doi.org/10.1146/annurev.micro.56.012302.160938>.
 36. Merz AJ, So M, Sheetz MP. 2000. Pilus retraction powers bacterial twitching motility. Nature 407:98–102. <https://doi.org/10.1038/35024105>.
 37. Maier B, Wong GC. 2015. How bacteria use type IV pili machinery on surfaces. Trends Microbiol 23:775–788. <https://doi.org/10.1016/j.tim.2015.09.002>.
 38. Okahashi N, Nakata M, Terao Y, Isoda R, Sakurai A, Sumitomo T, Yamaguchi M, Kimura RK, Oiki E, Kawabata S, Ooshima T. 2011. Pili of oral *Streptococcus sanguinis* bind to salivary amylase and promote the biofilm formation. Microb Pathog 50:148–154. <https://doi.org/10.1016/j.micpath.2011.01.005>.
 39. Moraes JJ, Stipp RN, Harth-Chu EN, Camargo TM, Höfling JF, Mattos-Graner RO. 2014. Two-component system VicRK regulates functions associated with establishment of *Streptococcus sanguinis* in biofilms. Infect Immun 82:4941–4951. <https://doi.org/10.1128/IAI.01850-14>.
 40. Okahashi N, Nakata M, Sakurai A, Terao Y, Hoshino T, Yamaguchi M, Isoda R, Sumitomo T, Nakano K, Kawabata S, Ooshima T. 2010. Pili of oral *Streptococcus sanguinis* bind to fibronectin and contribute to cell adhesion. Biochem Biophys Res Commun 391:1192–1196. <https://doi.org/10.1016/j.bbrc.2009.12.029>.
 41. Zuker M. 2003. Mfold web server for Nucleic acid folding and hybridization prediction. Nucleic Acids Res 31:3406–3415. <https://doi.org/10.1093/nar/gkg595>.